# Theory of dispersive shear Alfvén wave focusing in Earth's magnetosphere

R. Rankin, R. Marchand, J. Y. Lu, and K. Kabin
Department of Physics, University of Alberta, Edmonton, Alberta, Canada

V. T. Tikhonchuk
Centre Lasers Intenses et Applications, UMR 5107 CNRS - Université Bordeaux 1 - CEA, Université Bordeaux 1, Talence, France

Received 24 October 2004; revised 7 December 2004; accepted 28 December 2004; published 3 March 2005.

[1] It is shown that perpendicular gradients in shear Alfvén wave (SAW) dispersion regulate the localization of wave power on nightside geomagnetic $L$-shells where narrow Field Line Resonances (FLRs) form. We estimate the timescale for this process, $\omega_0 t_c = 1/\sqrt{|\beta|\alpha}$, and demonstrate that it is analogous to optical wave focusing. Here, $\beta$ is the gradient in the global wave dispersion parameter across $L$-shells in the equatorial plane, and $\alpha$ is the gradient in the SAW eigenfrequency. It is demonstrated that dispersive SAWs with wave numbers and frequencies in a certain range, are subject to magnetospheric focusing onto $L$-shells where they reach large amplitude and are expected to dissipate. Our theory addresses a class of arc scales that are comparable to the electron inertial length near the ionosphere, or the ion gyroradius near the equatorial plane. We further demonstrate that when the gradient in the SAW frequency reverses across the edges of auroral density cavities, it naturally traps dispersive SAWs and focuses them down to the inertial scale. **Citation:** Rankin, R., R. Marchand, J. Y. Lu, K. Kabin, and V. T. Tikhonchuk (2005), Theory of dispersive shear Alfvén wave focusing in Earth's magnetosphere, *Geophys. Res. Lett.*, *32*, L05102, doi:10.1029/2004GL021831.

## 1. Introduction

[2] The auroral zone supports low frequency (1–4 mHz) standing SAWs known as field line resonances (FLRs) [*Samson et al.*, 1991]. It is generally accepted that dispersive scale SAWs are necessary to explain acceleration of auroral electrons with energies up to several keV [*Lysak and Carlson*, 1981; *Thomson and Lysak*, 1996; *Chaston et al.*, 2003]. In SAWs, field-aligned currents and parallel electric fields produce electron precipitation through electron inertia and electron pressure [*Streltsov and Lotko*, 1996] terms in the generalized Ohm's law.

[3] In this paper, we demonstrate how narrow perpendicular scale standing SAWs might form in the inner magnetosphere, as a possible explanation of auroral arc formation in FLRs [*Samson et al.*, 1991]. FLRs may be stimulated through resonant mode conversion of fast mode surface waves excited by Kelvin-Helmholtz instabilities at the magnetopause [*Chen and Hasegawa*, 1974; *Southwood*, 1974; *Farrugia et al.*, 2000]. Other potential sources include solar wind pressure pulses that excite cavity or waveguide modes in the magnetosphere [*Samson et al.*, 1992; *Wright et al.*, 2002], or solar wind disturbances with frequencies matching FLR eigen-frequencies [*Rankin et al.*, 1993].

[4] Dispersive SAWs are discussed by *Rankin et al.* [1999], where it is demonstrated that wave dispersion is a global property of geomagnetic field lines, involving a weighted average of strongly varying electron inertia and thermal effects along field lines. In the nightside magnetosphere, inertial dispersion dominates field lines close to Earth, whereas at larger $L$-shells, thermal effects are dominant [*Streltsov and Lotko*, 1996]. This is described by the dispersion parameter $\delta$ (defined below) that changes from small negative, to large positive values, as a function of $L$. At locations where $\delta$ and its gradient across $L$ are small, FLRs reach their shortest scale. This happens because gradients in global wave dispersion rapidly defocus dispersive waves where thermal dispersion is large. This is important on field lines for which the timescale for linear wave phase mixing to the electron skin depth is large in comparison to the lifetime of FLRs [*Lu et al.*, 2003a].

## 2. Reduced-MHD Envelope Model for FLRs

[5] We shall investigate the properties of dispersive SAWs using the reduced-MHD envelope model of *Rankin et al.* [1999], which is valid provided the SAW amplitude and ambient plasma are slowly varying with respect to a wave period. The analysis is restricted to linear waves with small azimuthal wave number in the azimuthally symmetric magnetosphere. We can then write the slowly varying SAW magnetic field component as

$$h_\phi B_\phi = h_\phi^{eq} B_0^{eq} b(x,t) S_1(l) \exp i(m\phi - \omega_0 t)$$

where $h_\phi$ is the azimuthal metric coefficient in coordinates associated with the geomagnetic field, $B_0^{eq}$ is the ambient magnetic field strength at the equator, $S_1(l)$ is the SAW eigenfunction along the field line as defined by *Rankin et al.* [1999, equation (5)], and $b(x, t)$ is the slowly varying amplitude. The coordinate $l$ is measured along geomagnetic field lines with respect to the equator, while $x$ is the Earthward-directed perpendicular coordinate relative to a given magnetic field line at the equator. The choice of the envelope frequency $\omega_0$ is discussed below. Referring to


0094-8276/05/2004GL021831

*Rankin et al.* [1999], it is possible to write the evolution equation for $b(x, t)$ as,

$$\partial_t b - i\omega_0 \partial_x(\delta \partial_x b) = -i\Delta\omega b + \omega_0 R \quad (1)$$

Here, $\Delta\omega(x) = \omega_{SAW} - \omega_0$ is the ideal MHD eigenfrequency detuning across $L$-shells, and $R(x, t)$ is the amplitude of the SAW driver. Equation (1) is linear, with $\delta(x)$ defined by,

$$\delta = L^2 R_e^2 \int dl \left( \frac{3}{4} \frac{\rho_s^2}{\omega_0^2} \frac{V_A^2}{h_\mu} (\partial_l S_1)^2 + \frac{V_{Te}^2}{\omega_0^2 h_\mu} (\partial_l S_1) \partial_l (S_1 \lambda_e^2) - \frac{\lambda_e^2}{h_\mu} S_1^2 \right)$$

where $\rho_s$ is the ion acoustic gyroradius, $\lambda_e$ is the electron skin depth (inertial scale), $V_{Te}$ is the electron thermal speed, $h_\mu$ is the geomagnetic field-aligned metric coefficient, and the integral is taken over the total length of the magnetic field line. Equation (1) is derived from the wave equation for $B_\phi$ [see *Rankin et al.*, 1999, equation (4)], after substituting $h_\phi B_\phi$ defined above. The resulting expression is multiplied by the eigenfunction $S_1(l)$, and integrated along the field line to obtain equation (1). The second term in the integrand for $\delta$ corrects a typographical error in earlier publications ($S_1\lambda_e^2$ instead of $S_1^2\lambda_e^2$).

[6] The dispersion parameter $\delta(x)$ has three contributions, corresponding to finite ion acoustic gyroradius, electron temperature, and electron inertia, respectively. The two thermal contributions provide positive dispersion, while electron inertia gives a negative contribution. This designation refers to the sign of the group velocity, when computed from $\omega(x) \sim \Delta\omega(x) + \omega_0(1 + k_\perp^2\delta)$, which is valid in the WKB approximation. A convenient reference point $x = 0$ is the field line on which $\delta(x)$ vanishes and the SAW eigenfrequency is $\omega_0$. Then, we approximate the SAW frequency detuning and dispersion parameter with linear functions, $\Delta\omega(x) = \alpha\omega_0 x$ and $\delta(x) = \beta x$, respectively, where the gradients $\alpha$ and $\beta$ are characterized by ambient plasma parameters [see, e.g., *Lu et al.*, 2003a, Figure 9]. In the nightside magnetosphere, $\omega(x)$ increases toward Earth, so that $\alpha \sim R_e^{-1}$ is positive, while $\beta \sim -10^{-4}\ R_e$ is negative.

## 3. Qualitative Analysis of Perpendicular Gradients in SAW Dispersion

[7] First of all, we consider the condition for propagating waves to exist in the presence of gradients in global dispersion across geomagnetic field lines. We take $\alpha > 0$, and consider $\beta$ as either positive or negative. We assume also that dissipation can be represented by a step-like function, such that waves with $k_\perp > k_L$ are strongly damped. We will show below that the location $x = 0$ ($\delta = 0$) is an attractor for dispersive SAWs.

[8] Consider first $\beta > 0$. In the WKB approximation, propagating dispersive SAWs exist for $\alpha x < \omega\omega_0^{-1} - 1 < \alpha x + k_L^2\beta x$ if $x > 0$, and for $\alpha x > \omega\omega_0^{-1} - 1 > \alpha x + k_L^2\beta x$ if $x < 0$. This is shown in Figure 1a, where propagating waves exist within the hatched region on either side of the $\delta = 0$ field line (damping is represented by the dashed lines). The half-spaces $x < 0$ and $x > 0$ are decoupled, meaning that wave energy cannot pass from one half-space to the other. Each frequency on either side of the origin is different, and all waves impinge on the dissipation layer.

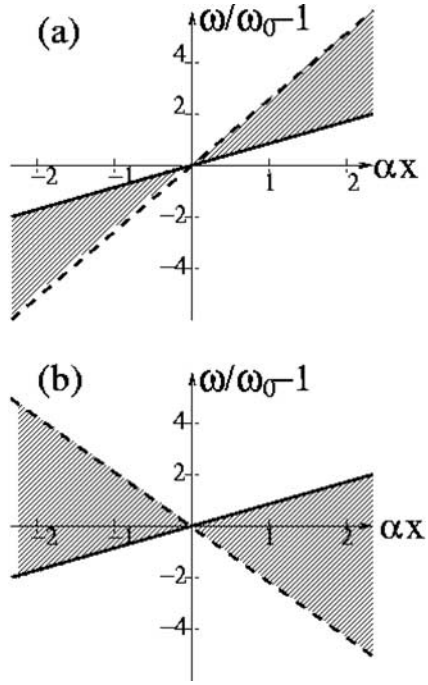


**Figure 1.** A schematic showing the domain in the ($\omega$, $x$) plane in which propagating SAWs can exist (shaded regions). The solid lines correspond to turning points where $k_\perp = 0$ or $\omega/\omega_0 - 1 = \alpha x$. The dashed lines correspond to the scale $k_L$ at which dissipation becomes important, $\omega/\omega_0 - 1 = (\alpha + k_L^2\beta)x$. (a) The case where the dispersion gradient $\beta$ is positive. (b) The more realistic situation in the magnetosphere where the dispersion gradient is negative.

This includes waves initially propagating away from $x = 0$, since they will reflect from their turning point where $k_\perp = 0$. The situation $\alpha\beta > 0$ is relevant to density cavities, where the gradient $\alpha$ reverses across the cavity. Dispersive waves are naturally trapped inside such cavities.

[9] Consider now the case $\beta < 0$. Propagating waves exist in the half-space $x > 0$ for $\alpha x > \omega\omega_0^{-1} - 1 > \alpha x + k_L^2\beta x$, and for $\alpha x < \omega\omega_0^{-1} - 1 < \alpha x + k_L^2\beta x$ for $x < 0$. Figure 1b shows that waves with the same frequency now exist on either side of $x = 0$, but waves with $\omega > \omega_0$ cannot reach this position from the right side (they are reflected at $k_\perp = 0$). Similarly, waves with $\omega < \omega_0$ cannot reach $x = 0$ from the left side. All other waves can propagate to $x = 0$, and therefore, the situation is similar to $\beta > 0$. We conclude that the location where $\delta(x)$ and its perpendicular gradient are close to zero act as an attractor for dispersive waves across a range of frequencies and wave numbers. Comparing the dispersion and inhomogeneity contributions in equation (1), one can estimate the spatial width of the resonance $\Delta x_c$ and the characteristic time of the resonance formation $t_c$:

$$\Delta x_c = \sqrt{|\beta|/\alpha}, \quad t_c = \left(\omega_0 \sqrt{|\beta\alpha|}\right)^{-1} \quad (2)$$

These estimates should ideally be evaluated at the dissipation layer using local field line parameters. Equation (2) can also be interpreted as space and timescales over which waves defocus on a given field line.

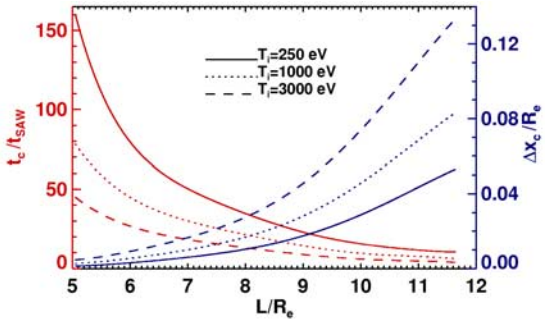


**Figure 2.** The figure shows the variation with equatorial distance of the characteristic spatial scale (scale on right and curves in blue) and the characteristic timescale (scale on left and curves in red) for defocusing on a given geomagnetic field line. The Tsyganenko 1996 geomagnetic field model is used, with solar wind pressure $P = 1$ nPa, $Dst = -10$ nT, $B_y = 0$, and $B_z = -1$ nT. The plasma sheet density is 0.5 cm$^{-3}$. Constant pressure along geomagnetic field lines is assumed with $T_e = 250$ eV at the equator, and ion temperatures as indicated on the figure.

[10] Figure 2 shows the $L$-shell variation of the space and time scales defined by equation (2) for quiet solar wind conditions. The Tsyganenko 1996 model is used, with solar wind pressure $P = 1$ nPa, $Dst = -10$ nT, $B_y = 0$, and $B_z = -1$ nT. The defocusing time and spatial width have an inverse relationship, and both are strongly varying through the night-side plasma sheet. In the case of hot plasma, beyond $L \sim 12$, $t_c$ becomes comparable to the SAW eigenfrequency, and the envelope approximation is no longer valid. Note that equation (2) is only an estimate of effects of dispersion gradients. The analysis and numerical results below indicate a faster evolution (see Figure 3, for example).

## 4. Quantitative Analysis

[11] The tendency for global (i.e., whole field line) wave energy to focus Earthward onto field lines where wave dispersion is small, can be analyzed using a Fourier Transform and Green's function approach. The analysis is straightforward, but only the essential results are presented. To understand the evolution of the shear wave amplitude, consider a Gaussian wave-packet of width $\Delta x_0$ that is excited at some equatorial position $x_0$. An impulse $R(x, t) = R_0 \exp(ik_0 x) g[(x - x_0)/\Delta x_0]\delta_D(t)$ is applied, with $\delta_D(t)$ the Dirac delta-function, $R_0$ the amplitude of the driver, and $g(x) = (2\pi)^{-1/2}\exp(-x^2/2)$. Assuming that $k_0\Delta x_0 \gg 1$, it can be shown that a particular wave number $k_m(t)$ dominates the Green's function for $b(x, t)$. This allows us to write the analytic solution in the form defined by,

$$b(x,t) \sim \frac{1}{\partial_{k_\perp} K} \exp\left( ik_m(t)x + \beta\omega_0 \int_0^t dt' k_m(t') \right) g[(x - x_m)/\Delta x_m],$$

where $x_m(t) = x_0 \partial_{k_\perp} K|_{k0}$ is the position of the center of the wave-packet, and $\Delta x_m(t) = \Delta x_0 \partial k_\perp K|_{k0}$ is its width. Here, $K(k_\perp,t)$ is the solution to the characteristic equation $dk_\perp/dt = -\omega_0(\alpha + \beta k_\perp^2)$, with initial condition $K(k_\perp,0) = k_\perp$. The dominant wave number $k_m(t)$ of the wave packet is defined by $K(k_m(t),t) = k_0$. We note that $K(k_\perp,t)$ depends on the relative sign of the parameters $\alpha$ and $\beta$. The case corresponding to $\beta > 0$ has solutions defined by,

$$K(k_\perp, t) = k_c \tan\left[ \arctan\frac{k_\perp}{k_c} - \frac{t}{t_c} \right] \tag{3}$$

where $k_c = 1/\Delta x_c$ and $t_c$ are two convenient scale parameters defined by equation (2). The case corresponding to $\beta < 0$ has two branches for the characteristics that are defined by,

$$\begin{aligned} K_<(k_\perp, t) &= k_c \tanh\left[ \operatorname{arctanh}\left(\frac{k_\perp}{k_c}\right) - \frac{t}{t_c} \right], \\ K_>(k_\perp, t) &= k_c \coth\left[ \operatorname{arccoth}\left(\frac{k_\perp}{k_c}\right) - \frac{t}{t_c} \right]. \end{aligned} \tag{4}$$

The first definition in equation (4) is valid for $|k_\perp| < k_c$ whereas the second definition is valid for $|k_\perp| > k_c$. The behavior of the wave-packet is determined by the derivative $\partial_{k\perp}K$ that defines its position and width as a function of time. It can be shown that the required derivative is $\partial_{k\perp}K = (k_0^2 + k_c^2)/(k_m^2(t) + k_c^2)$ for $\beta > 0$ and $\partial_{k\perp}K = (k_0^2 - k_c^2)/(k_m^2(t) - k_c^2)$ for $\beta < 0$.

[12] When $\beta > 0$, equation (3) shows that irrespective of the initial wave number $k_0$ the dominant mode $k_m(t)$ diverges to infinity after a time $t = t_c[\pi/2 - \arctan(k_0/k_c)]$. Correspondingly, its width approaches zero and its position terminates on the $\delta = 0$ field line in the absence of dissipation. This is shown in Figure 3a, and corresponds to focusing of waves with all frequencies onto the location $\delta = 0$. Alternatively, any perturbation created at an arbitrary

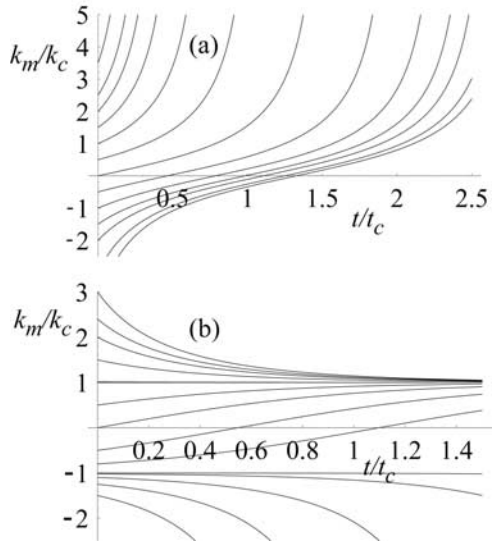


**Figure 3.** The figure shows the temporal evolution of the wave number $k_m(t)$ characterizing a spatial wave packet in the WKB approximation. The axes are normalized by the scales defined in equation (2). (a) The situation where the dispersion gradient $\beta$ is positive. (b) The more realistic situation in the magnetosphere where the dispersion gradient is negative. The normalization factor $k_c = 1/\Delta x_c$ is defined by the quantity in equation (2).

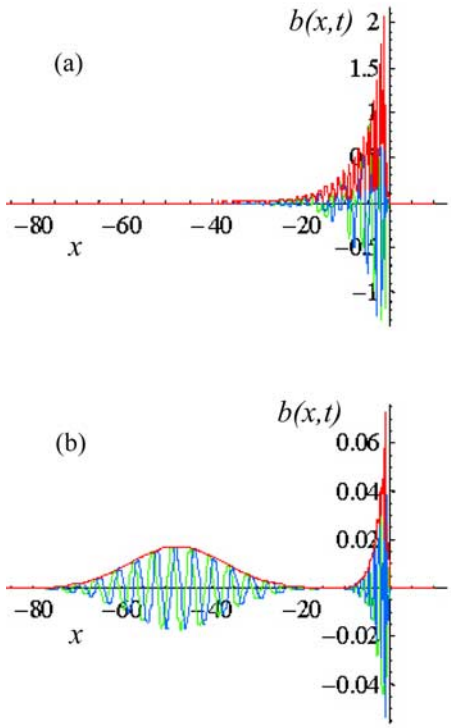


**Figure 4.** The figure shows the spatial distribution of the wave field (in arbitrary units) near the zero dispersion line for the case of (a) a wavepacket impulse and (b) a wavepacket excited by a continuous driver. The spatial scale is in units of parameter $\Delta x_c$ introduced in the text. The case shown corresponds to negative $\beta$; the green and blue curves correspond to the real and imaginary parts of $b$, while the red line gives its absolute value. The source is located at $-50\ \Delta x_c$ and has a width of $10\ \Delta x_c$.

position $x_0$ can be said to defocus and run away from where it is excited after a time $\pi t_c$. Obviously, one should account for dissipation if the wave number $k_m$ exceeds the cut-off wave number $k_L$, but this is outside the scope of the present analysis [*Tikhonchuk and Rankin*, 2002; *Lysak and Song*, 2003].

[13] The case with $\beta < 0$ is illustrated by Figure 3b. In this case, waves with initial perpendicular wave numbers satisfying $k_0 < -k_c$ become trapped at $x = 0$ after a time $t = t_c \text{arctanh}(k_c/k_0)$. This is similar to the previous case with $\beta > 0$. However, all of the characteristics emanating from $k_0 > -k_c$ approach $k_c$ asymptotically in time. Correspondingly, such waves propagate to infinity with decreasing (increasing) amplitude (width). Thus, for this range of wave numbers, wave-packets are able to escape from the $\delta = 0$ location. We note also that for $k_0 > k_c$, waves initially move toward the $\delta = 0$ location, but are reflected from turning points at $x = x_0(1 - k_0^2/k_c^2)$ before propagating away to infinity.

[14] The analysis discussed above is confirmed by numerical solutions to equation (1). Figure 4 shows the accumulation of wave energy near $\delta = 0$ for a pulse launched at time $t = 0$ (a) and a constant driver (b). In both cases the wave approaches the point $x = 0$ and stays there for a time of the order of $t_c$. Note that without accounting for dispersion gradients, the initial wave disturbance would phase mix at the location where it is excited. On low $L$-shells, the "dwell time" $t_c$ exceeds the lifetime of observed FLRs, and thus the associated inertial scale waves have sufficient time to energize auroral electrons and dissipate.

## 5. Conclusions

[15] Observations suggest that a certain class of discrete arcs is associated with FLRs on low $L$-shells down to $L \sim 6$ (assuming a dipolar field). The observed range of night-side latitudes for FLRs is generally attributed to mode conversion of monochromatic (1–4 mHz) fast mode Alfvén waves with frequencies matching the local SAW eigenfrequency. However, plasma on night-side field lines is relatively hot, making it difficult to form inertial scale FLRs because of the temperature dependence of the global properties of wave dispersion.

[16] We have demonstrated that thermal (perpendicular) gradients in global (whole field line) wave dispersion produce focusing of SAWs into the night-side inner magnetosphere. This does not require a monochromatic driver, although stretched fields and the associated slow variation of the eigenfrequency across $L$-shells, should lend itself to more efficient coupling at the dissipation layer (see *Lu et al.* [2003a, Figure 8], which shows numerical solutions to the non-perturbative reduced MHD equations). Equation (2) shows that at such locations, very short perpendicular scale structures should naturally form [*Streltsov and Lotko*, 1996]. Since the perpendicular group velocity of dispersive SAWs is small at such locations, SAW ponderomotive forces may steepen the Alfvén speed gradient [*Lu et al.*, 2003b]. This should further decrease FLRs widths by focusing them into density cavities.

[17] One speculative aspect of our analysis, is that while global fast mode waves may often be present, they will not couple efficiently to discrete FLRs unless the phase mixing time is comparable to $t_c = (\omega_0\sqrt{|\beta|\alpha})^{-1}$ where $t_c$ is the defocusing timescale, $\alpha$ is the gradient scale for the SAW frequency, and $\beta$ is the corresponding gradient in SAW dispersion on a given geomagnetic field line.

[18] **Acknowledgment.** The authors acknowledge the support of the Natural Sciences and Engineering Research Council of Canada (NSERC) and the Canadian Space Agency.

## References

Chaston, C. C., J. W. Bonnell, C. W. Carlson, J. P. McFadden, R. J. Strangeway, and R. E. Ergun (2003), Kinetic effects in the acceleration of auroral electrons in small scale Alfven waves: A FAST case study, *Geophys. Res. Lett.*, *30*(6), 1289, doi:10.1029/2002GL015777.

Chen, L., and A. Hasegawa (1974), A theory of long period magnetic pulsations: 2. Impulse excitation of surface eigenmode, *J. Geophys. Res.*, *79*, 1033.

Farrugia, C. J., et al. (2000), Coordinated Wind, Interball/tail and ground observations of Kelvin-Helmholtz waves at the near-tail, equatorial magnetopause at dusk: January 11, 1997, *J. Geophys. Res.*, *105*, 7639.

Lu, J. Y., R. Rankin, R. Marchand, and V. T. Tikhonchuk (2003a), Finite element modelling of dispersive field line resonances: Trapped shear Alfven waves inside field-aligned density structures, *J. Geophys. Res.*, *108*, 1394, doi:10.1029/2003JA010035.

Lu, J. Y., R. Rankin, R. Marchand, and V. T. Tikhonchuk (2003b), Nonlinear acceleration of dispersive effects in field line resonances, *Geophys. Res. Lett.*, *30*, 1540, doi:10.1029/2003GL016929.

Lysak, R. L., and C. W. Carlson (1981), Effect of microturbulence on magnetosphere-ionosphere coupling, *Geophys. Res. Lett.*, *8*, 269.

Lysak, R. L., and Y. Song (2003), Nonlocal kinetic theory of Alfvén waves on dipolar field lines, *J. Geophys. Res.*, *108*(A8), 1327, doi:10.1029/2003JA009859.

Rankin, R., J. C. Samson, and P. Frycz (1993), Simulations of driven field line resonances in Earth's magnetosphere, *J. Geophys. Res.*, *98*, 21,341.

Rankin, R., J. C. Samson, V. T. Tikhonchuk, and I. Voronkov (1999), Auroral density fluctuations on dispersive field line resonances, *J. Geophys. Res.*, *104*, 4399.

Samson, J. C., T. J. Hughes, F. Creutzberg, D. D. Wallis, R. A. Greenwald, and J. M. Ruohoniemi (1991), Observations of a detached, discrete arc in association with field line resonances, *J. Geophys. Res.*, *96*, 15,683.

Samson, J. C., B. G. Harrold, J. M. Ruohoniemi, R. A. Greenwald, and A. D. M. Walker (1992), Field line resonances associated with MHD waveguide modes in the magnetosphere, *Geophys. Res. Lett.*, *19*, 441.

Southwood, D. J. (1974), Some features of field line resonances in the magnetosphere, *Planet. Space Sci.*, *22*, 483.

Streltsov, A., and W. Lotko (1996), The fine scale structure of dispersive, non-radiative, field line resonances, *J. Geophys. Res.*, *100*, 5343.

Thomson, B. J., and R. L. Lysak (1996), Electron acceleration by inertial Alfven waves, *J. Geophys. Res.*, *101*, 5359.

Tikhonchuk, V. T., and R. Rankin (2002), Parallel potential driven by a kinetic Alfvén wave on geomagnetic field lines, *J. Geophys. Res.*, *107*(A7), 1104, doi:10.1029/2001JA000231.

Wright, A. N., K. J. Mills, A. W. Longbottom, and M. S. Ruderman (2002), The nature of convectively unstable waveguide mode disturbances on the magnetospheric flanks, *J. Geophys. Res.*, *107*(A9), 1242, doi:10.1029/2001JA005091.

K. Kabin, J. Y. Lu, R. Marchand, and R. Rankin, Department of Physics, University of Alberta, Edmonton, AB, Canada T6G 2J1. (rankin@space.ualberta.ca)

V. T. Tikhonchuk, Centre Lasers Intenses et Applications, UMR 5107 CNRS - Université Bordeaux 1 - CEA, Université Bordeaux 1, F-33405 Talence Cedex, France.